Mini-stopbands of a one-dimensional system: The channel waveguide in a two-dimensional photonic crystal

S. Olivier, M. Rattier, H. Benisty, and C. Weisbuch
Laboratoire Physique de Matiére Condensée, Ecole Polytechnique, 91128 Palaiseau Cedex, France

C. J. M. Smith and R. M. De La Rue
Optoelectronics Research Group, University of Glasgow, Glasgow G12 8LT, Scotland

T. F. Krauss
School of Physics and Astronomy, University of St. Andrews, St. Andrews KY16 9SS, Scotland

U. Oesterle and R. Houdré
Institut de Micro- et Opto-électronique, Ecole Fédérale de Lausanne, CH-1025 Lausanne, Switzerland
(Received 5 September 2000; published 1 March 2001)

We show that a channel waveguide in a two-dimensional photonic crystal channel can be considered as a periodic one-dimensional system. Waveguides were fabricated into a $GaAs/Al_xGa_{1-x}As$ waveguide heterostructure and the waveguide transmission was measured by detecting the guided photoluminescence of embedded InAs quantum dots excited near the guide entrance. Mini-stopbands related to anticrossings in the dispersion were observed and the spectral location and width of these transmission stopbands is found to agree well with calculated values.

DOI: 10.1103/PhysRevB.63.113311 PACS number(s): 42.82.Bq, 42.82.Et, 42.82.Gw

The study of wave transmission through periodic structures goes back to the turn of the last century. The basis of our modern understanding of periodic structures was laid by Brillouin[1] and has been applied across many domains of physics: solid-state, optics, mechanics, etc. Periodicity, however, has a special role when discrete modes, as opposed to the continuum, are involved, as is the case in waveguides. A perfect, lossless, planar metallic waveguide, whose dispersion relation $\omega(k_{\|})$ is sketched in Fig. 1(a), is an ideal system to introduce the main concept of the discretization of the radiation continuum and the effect of periodic features in the guide. Each branch has a cutoff frequency that is determined by the guide thickness (field conservation requires the electric field to be zero at the metal boundaries) and so, for a given guide thickness, there are a defined number of modes per polarization. Generally speaking, if a periodic perturbation is introduced, e.g., a thickness variation of period a, then mode coupling between modes i and j will occur whenever the two wave vectors along the direction of propagation differ by an integer number of reciprocal lattice vectors.

As can be seen on Fig. 1(a), there are diagonal couplings $(i=j)$ at the zone boundaries $(k_{\|}=\pi/a)$. At this point, the two counterpropagating waves form a standing wave pattern and a gap opens, namely, the text book situation that gives rise to the electronic forbidden bands. In optics, it gives rise to photonic band gaps;[2,3] in one dimension, a simple multilayer stack of alternate indices, also known as a distributed Bragg reflector (DBR) is the best known example. There are, however, off-diagonal couplings, $i \neq j$, which do not occur at the zone boundaries. It is the purpose of this report to show the phenomena stemming from the existence of these off-diagonal couplings in a channel waveguide defined in a two-dimensional photonic crystal (PC) [(Fig. 1(b)].[4,5] Photonic crystals are periodic optical structures on the length scale of the electromagnetic wavelength that, under the correct conditions, produce photonic band gaps (PBG), namely spectral regions of forbidden propagation. This key property creates the possibility to realize novel guides with minimal losses at sharp bends (radii on the scale of the wavelength of light).[6] The reasons for the present study can be addressed from, first, the application of photonic crystals as transverse boundaries to otherwise planar waveguides or, second, the introduction of defects into photonic crystals.

In the former approach, the band gap of the photonic crystal guaranteed the existence of guided modes with any value of $k_{\|}$, at variance with the more usual index confinement for which only a limited range of wave vectors are localized (as allowed by total internal reflections at the core/cladding interfaces). In other words, the PC boundaries provide similar confinement to that provided by a perfect metal, even though it is a patterned dielectric. It should be noted that a conventional index-guided waveguide with a similar periodic corrugation would give rise to radiation to the continuum rather than pure off-diagonal couplings as the in-plane confinement is not omnidirectional and the corrugation opens a scattering path.

In the second approach, one is interested in the intrinsic properties of line defects created in two-dimensional (2D) photonic crystals. In the direction of propagation, the system has the periodicity of the crystal while this periodicity is broken in the transverse direction [Fig. 1(b)]. It is this local breaking of the symmetry that provides the physical phenomena that are used for so many applications, e.g., dopant atoms in semiconductor lattices and dislocations. The same is true for light confinement by defects in photonic crystals.

Note two simple ideas: first, if the guide is very thin [i.e., if the guide of Fig. 1(b) is very narrow], then the cutoff of

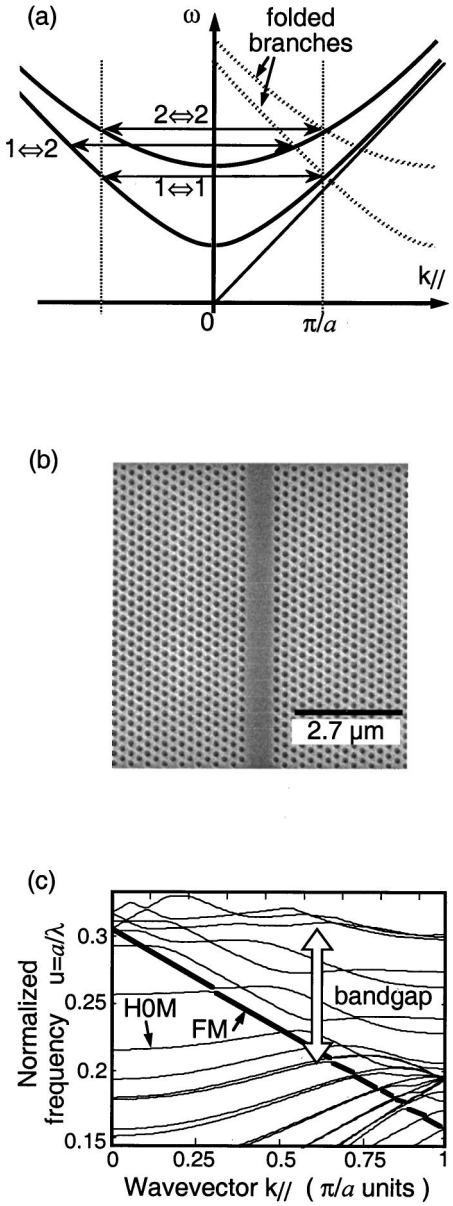

FIG. 1. (a) Dispersion relation for an ideal metal waveguide; (b) SEM micrograph of the photonic crystal channel waveguide *W*3; (c) calculated dispersion relations for *W*3 in TE polarization (parameters given in text).

the second mode may lie above the PBG and no off-diagonal coupling can occur due to the breakdown of confinement; second, in this configuration the photonic crystal dictates both the working range of frequencies (PBG)—the vertical axis of Fig. 1(a)—and the periodicity of the waveguide—the Brillouin-zone boundary.

We will first detail the role of the dimensionality of our system and, in particular, why our 3D system (2D photonic crystal patterned into a monomode slab waveguide) can be considered quasi-2D. We next present a theoretical account of the dispersion relations of modes in a PC channel waveguide demonstrating the crossings and anticrossings of the guided modes. This theoretical description is then confirmed by experimental transmission measurements at near-infrared wavelengths.

In the report presented here, we are dealing with a 3D system, namely a $GaAs/Al_xGa_{1-x}As$ planar waveguide, that provides ''weak'' index guiding in the out-of-plane (vertical) direction, into which a 2D triangular array of air holes is patterned [Fig. 1(b)]; weak guiding means that the difference in the refractive index between the core and cladding regions is typically less than unity (in detail, the heterostructure features a 400 nm-thick $Al_{0.8}Ga_{0.2}As$ bottom cladding, a 220 nm-thick GaAs core and a 310 nm-thick $Al_{0.8}Ga_{0.2}As$ top cladding, hence indices at 1000 nm 3.1/3.5/3.4, respectively). In such a system, there is not a complete confinement of the light in three dimensions and so the holes represent a mechanism for radiation losses out of the plane of the slab waveguide. The authors have shown over recent years, however, that this particular structure can be considered as a 2D system. This has been demonstrated by the measured high reflectivities in the 2D stopbands, high transmission in the passbands[7–9] and the high-finesse resonances of PC-based microcavities.[9–11] The corrections to the 2D picture are modest in the regime of ''weak'' guiding that is considered here and have been addressed in the literature.[12] Recently, some of the authors introduced a scheme whereby these losses intrinsic to such a system can be treated in two dimensions by a variable separable approach.[13] It should be noted that ''strong'' vertically index guided structures require a thorough 3D treatment[14,15] but we do not consider this case here. In summary, we may treat our system as a 2D one, with a matrix index equal to the effective index $n_{\mathrm{eff}}=3.32$ of the planar waveguide mode, and still $n=1$ in air.

The calculation of the dispersion relations for the 2D photonic crystal waveguide (PC-WG) is conveniently achieved numerically by the supercell method.[16] As there is still a periodicity in the direction of propagation, the wave vector in this direction is well defined. The base set of parameters are the matrix dielectric constant $\epsilon_m(\equiv n_{\mathrm{eff}}^2)$ and the air-filling fraction $f=(2\pi/\sqrt{3})a^2/r^2$ in a triangular lattice. A channel PC-WG, denoted *Wn*, is defined by removing *n* dense (10) rows; in this report we consider only propagation along this direction. For odd values of *n*, the guide is symmetric with respect to the mirror plane in the center of the guide, but note that for even values of *n*, this is no longer the case [Fig. 1(b)]. These two guides are denoted *A* type (symmetric) and *B* type as in earlier work.[16] For *B* type, an additional $a/2$ shift along the guide is required to transform one of the boundaries to the other. There are intermediate cases between these extremes with less symmetry, and hence, more complicated band structures.

The calculation of the dispersion of *W*3 is given in Fig. 1(c) ($\epsilon_m=11$, $f=37\%$) for the TE polarization for which the in-plane band gap covers the range of normalized frequencies $u=a/\lambda$ from 0.22 to 0.31. The thick line is the fundamental mode (FM). Apart from folding at $k_{\|}=\pi/a$, the dispersion relation of the FM is very close to the bulk matrix dispersion $\omega^2=\epsilon_m k_{\|}^2/c^2$. This is because the penetration of the fundamental mode, in the TE gap, is much less than the width of *W*3, so that the FM field is essentially localized in the waveguide core. We see many higher-order modes (HOM's) with parabolic dispersion $u_{\mathrm{HOM}}(k_{\|})$ around $k_{\|}=0$. These modes are similar to the Fabry-Perot (FP) modes stud-

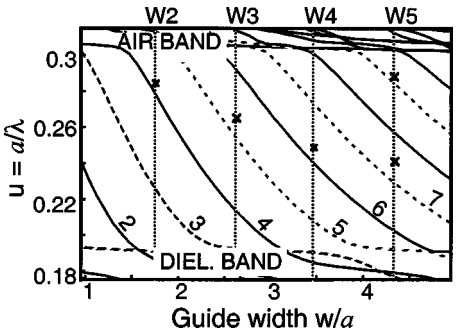

FIG. 2. (a) Plot of $k_{\|}=0$ frequencies of PC-WG's as a function of their normalized width. The continuous lines correspond to odd modes whereas the dashed lines correspond to even modes. Experimental frequencies of the mini-stopbands for the guides $W2$, $W3$, $W4$, $W5$ are given by the crosses.

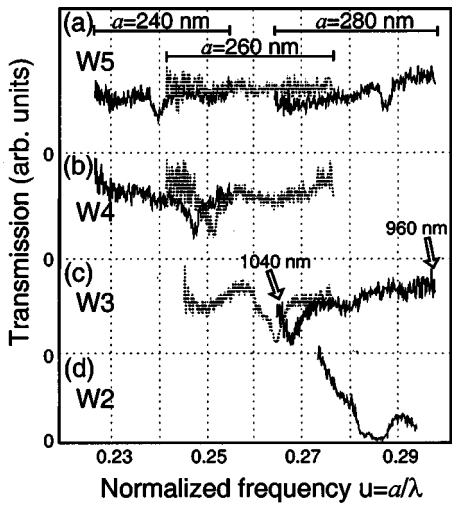

FIG. 3. Experimental transmissions for various waveguide widths as a function of the normalized frequency $u=a/\lambda$: (a) ($W5$, $a=240$ nm), ($W5$, $a=260$ nm), and ($W5$, $a=280$ nm); (b) ($W4$, $a=240$ nm) and ($W4$, $a=260$ nm); (c) ($W3$, $a=260$ nm) and ($W3$, $a=280$ nm); (d) ($W2$, $a=280$ nm).

ied in Ref. 9, except that in the reported study, the PC's on either side were only four rows thick and only $k_{\|}=0$ (normal incidence) was reported. We will, for this reason, denote below FP resonances the normalized frequencies $u_{\mathrm{HOM}}(k_{\|}=0)$.

It should be noted that the guidance of HOM's at small $k_{\|}$ relies completely on Bragg reflection at the PC walls, in contrast to ordinary index waveguides, whereas the FM tends to be guided by the average index difference between the bulk core and the PC claddings. This ''index'' guiding is to be expected at frequencies below the band gap: in this long-wavelength limit, the lower effective average index in the PC provides the necessary lateral confinement.

In Fig. 1(c) it can be seen that there are crossings and anticrossings of the guided modes. It was noted in Ref. 15 that the diagonal couplings (at $k_{\|}=\pi/a$) are allowed for A- and forbidden for B-type guides, hence modes of same parity are necessary for coupling in A type. The same kind of symmetry considerations applies here to all couplings, although the symmetry operation is not just parity as we work in the middle of the Brillouin Zone. As a result, only each other HOM can couple to the FM. For A-type guides, these are the HOM's corresponding to even FP modes, and conversely, for B-type guides, the HOM's coupled to the FM correspond to odd FP modes. Note also that anticrossings may occur between, say, the second mode and every other HOM with similar rules.

The spectral location of the mini-stopbands MSB's results from the specific HOM and FM dispersion relations. However, one simple feature in Fig. 1(c) is that the spectral position of MSB's is dictated to a large degree by the FP resonances $u_{\mathrm{HOM}}(k_{\|}=0)$, insofar as MSB's occur at small $k_{\|}$, which will be the case for large u values close to the crystal upper band-gap edge. We expect, on the other hand, that close to the low-frequency edge, the anticrossing occurs at larger $k_{\|}$, hence at a value of u, substantially larger than the FP resonance $u_{\mathrm{HOM}}(k_{\|}=0)$. So, predicting the occurrence of MSB's basically amounts to tracking the FP frequencies. This greatly reduces the computational task as one avoids the painful examination of band diagrams for each value of the guide width. The result is the plot of Fig. 2 giving these FP frequencies $u_{\mathrm{HOM}}(0)$ for the A- and B-type guides as a function of their normalized width w/a.

Let us now turn to the experiments (crosses on Fig. 2, see below). The PC-WG's were fabricated using a combination of electron-beam lithography and reactive-ion etching, as detailed elsewhere.[17] The final etch depth of the holes was 0.7 μm, a depth sufficient to overlap with the guided mode—a necessary requirement for photonic bandgap behavior in these structures.[13,18] The $GaAs/Al_xGa_{1-x}As$ waveguide is identical to that used previously[9] and comprises a 0.24 μm thick GaAs core with an $Al_{0.2}Ga_{0.8}As$ upper and an $Al_{0.8}Ga_{0.2}As$ lower cladding. In the core, three layers of InAs self-organized quantum dots were grown and are used as a broadband internal luminescence source for the experiments.[19] The photoexcitation spot is located at the guide entrance, so that the fundamental mode of the PC-WG is primarily what we excite, for symmetry reasons. As in Ref. 19, light coming out of the PC-WG at a cleaved facet normal to guide axis is imaged onto a charge-coupled device (CCD) camera. In order to ensure that we measure the signal from the guide, we focus inside the planar waveguide to the virtual focus of the PC-WG exit, at which astigmatism leads to a spot shape normal to the cleaved edge.[20] Two identical patterns located at different distances from the cleaved edge, and for which measurements are made at the adequate, but different internal focal points, are used to double check these measurements. In order to obtain more quantitative features associated with the waveguide transmission and take out the source spectrum, we ratio the bare waveguide transmission spectrum, $I(\lambda)$, with a spectrum from an unpatterned area $I_0(\lambda)$ taken at the same distance from the cleaved edge, thereby eliminating absorption in the guide plane.[19] More thorough quantitative measurements on propagation losses of these waveguides will be presented elsewhere.[21]

With this method, Fig. 3 shows experimental transmissions for the 30 rows long PC-WG in the following cases

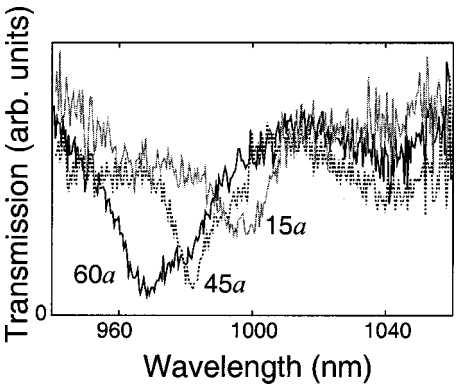

FIG. 4. Transmission along 15, 45, and 60 row long $W3$ guides for the period $a=260$ nm showing the effect of guide length.

(a) ($W5$, $a=240$ nm), ($W5$, $a=260$ nm), and ($W5$, $a=280$ nm); (b) ($W4$, $a=240$ nm) and ($W4$, $a=260$ nm); (c) ($W3$, $a=260$ nm) and ($W3$, $a=280$ nm); (d) ($W2$, $a=280$ nm). In all these cases, MSB's are clearly seen (in the case of $W1$, we did not have enough signal, probably due to the small intrinsic coupling of the internal source to this narrow guide). The central wavelengths of these anticrossings are plotted as crosses on Fig. 2. We remind that, to compare the 2D calculation to experiments, one should use for ϵ_m the squared effective index n_{eff}^2. Material dispersion is here primarily responsible for a shift from $\epsilon=11.3$ to $\epsilon=11.9$ when going from 1080 nm to 940 nm, with secondary corrections arising from modal dispersion. Part of the mismatch between the two spectra in (b) and in (c) stems from dispersion, the rest from small fluctuations in fabrication. The positions of the observed MSB's (crosses on Fig. 2) are in excellent agreement with the calculated FP frequencies at large frequencies. At lower frequencies, we checked using the full dispersion calculation that the shift in Fig. 2 indeed came from the HOM dispersion relation (as discussed in the theoretical section above), and that the excellent agreement between experimental and theoretical positions for the MSB's is also observed at lower frequencies.

In Fig. 4, we have superimposed the ratio $I(\lambda)/I_0(\lambda)$ for $W3$ ($a=260$ nm) and $L=15$, 45, 60, which shows the steady decrease of transmission at the MSB dip T_{min}. The value of T_{min} is compatible with those of ordinary DBR's (counterpropagative coupling, be it in a multilayer stack or in a corrugated waveguide) in which a 1% stop band over, e.g., 60 periods corresponds to the classical quantity $\kappa L=0.94$ (where κ is the coupling constant of a coupled-mode theory familiar to practitioners in the field,[22] and L the length) and leads to $T_{\mathrm{min}}=1-\coth(\kappa L)=0.26$ of the same order. The correlation between spatial decay of the incoming mode and stop-band width seems, therefore, to be the same in the present system and in ordinary DBR's.

In conclusion, using a channel PC waveguide patterned in a conventional semiconductor heterostructure to freeze the third dimension, we have clearly demonstrated a characteristic property of discrete modes in a one-dimensional periodic system: the appearance of nondiagonal couplings and associated mini-stopbands. Their occurrence has been traced to the successive Fabry-Perot modes of the PC-WG: once they acquire an adequate momentum along the guide, they can couple to the fundamental mode through the periodic corrugation if symmetry allows. Their spectral location was found to agree very well with theory for a large number of different widths and periods. The calculated minigap spectral width is in agreement with the MSB's observed width, and the rate of extinction is in agreement with what can be expected for similar DBR's. We thus find that the strong modulation of the basic crystal (large band gap) translates into much finer structures on the few discrete modes that are introduced along a line defect of a few missing rows.

[1] L. Brillouin, *Wave Propagation in Periodic Structures* (Dover, New York, 1953).
[2] E. Yablonovitch, Phys. Rev. Lett. **58**, 2059 (1987).
[3] J. D. Joannopoulos, R. D. Meade, and J. N. Winn, *Photonic Crystals, Molding the Flow of Light* (Princeton University, Princeton, NJ, 1995).
[4] T. Baba, N. Fukaya, and J. Yonekura, Electron. Lett. **35**, 654 (1999).
[5] M. Tokushima, H. Kosaka, A. Tomita, and H. Yamada, Appl. Phys. Lett. **76**, 952 (2000).
[6] R. D. Meade *et al.*, J. Appl. Phys. **75**, 4753 (1994).
[7] D. Labilloy *et al.*, Phys. Rev. B **59**, 1649 (1999).
[8] D. Labilloy *et al.*, Phys. Rev. Lett. **79**, 4147–4150 (1997).
[9] H. Benisty *et al.*, J. Lightwave Technol. **17**, 2063 (1999).
[10] C. J. M. Smith *et al.*, IEE Proc.: Optoelectron. **145**, 373 (1998).
[11] C. J. M. Smith *et al.*, Electron. Lett. **35**, 228 (1999).
[12] V. N. Astratov *et al.*, J. Lightwave Technol. **17**, 2050 (1999).
[13] H. Benisty *et al.*, Appl. Phys. Lett. **76**, 532 (2000).
[14] P. S. J. Russell, D. A. Atkin, T. A. Birks, and P. J. Roberts, in *Microcavities and Photonic Bandgaps: Physics and Applications*, edited by J. Rarity and C. Weisbuch (Kluwer, Dordrecht, 1996), pp. 203–218.
[15] S. G. Johnson, S. Fan, P. R. Villeneuve, J. D. Joannopoulos, and L. A. Kolodziejski, Phys. Rev. B **60**, 5751 (1999).
[16] H. Benisty, J. Appl. Phys. **79**, 7483 (1996).
[17] T. F. Krauss *et al.*, Microelectronics **35**, 29 (1997).
[18] T. F. Krauss and R. M. De La Rue, Appl. Phys. Lett. **68**, 1613 (1996).
[19] D. Labilloy *et al.*, Appl. Phys. Lett. **71**, 738 (1997).
[20] C. J. M. Smith *et al.*, *Quantitative and Qualitative Analysis of 2D Photonic Crystal Waveguides*, PECS, Sendai (Japan), March 3-8 (RIEC, Tohoku University, 2000).
[21] C. J. M. Smith *et al.*, Appl. Phys. Lett. **77**, 2813 (2000).
[22] *Guided Wave Optoelectronics*, edited by T. Tamir (Springer-Verlag, Berlin, 1990), Vol. 26.